Breaking Down Monocular Ambiguity: Exploiting Temporal Evolution for 3D Lane Detection

Huan Zheng*, Wencheng Han*, Tianyi Yan, Cheng-zhong Xu, Jianbing Shen[†] SKL-IOTSC, CIS, University of Macau

Abstract

Monocular 3D lane detection aims to estimate the 3D position of lanes from frontal-view (FV) images. However, existing methods are fundamentally constrained by the inherent ambiguity of single-frame input, which leads to inaccurate geometric predictions and poor lane integrity, especially for distant lanes. To overcome this, we propose to unlock the rich information embedded in the temporal evolution of the scene as the vehicle moves. Our proposed Geometryaware Temporal Aggregation Network (GTA-Net) systematically leverages the temporal information from complementary perspectives. First, Temporal Geometry Enhancement Module (TGEM) learns geometric consistency across consecutive frames, effectively recovering depth information from motion to build a reliable 3D scene representation. Second, to enhance lane integrity, Temporal Instance-aware Query Generation (TIQG) module aggregates instance cues from past and present frames. Crucially, for lanes that are ambiguous in the current view, TIQG innovatively synthesizes a pseudo future perspective to generate queries that reveal lanes which would otherwise be missed. The experiments demonstrate that GTA-Net achieves new SoTA results, significantly outperforming existing monocular 3D lane detection solutions.

1. Introduction

Monocular 3D lane detection, the task of estimating the precise 3D coordinates of lane lines from a single camera, is a cornerstone of modern autonomous driving systems [31]. Accurate 3D lane perception is crucial for safe lane keeping [41], as well as for downstream tasks like high-definition map construction [19, 26] and trajectory planning [45]. While cost-effective and rich in texture, monocular vision presents a formidable challenge: how to recover 3D structure from a 2D image.

Existing methods attempt to bridge this 2D-to-3D gap through various strategies, such as two-stage projection

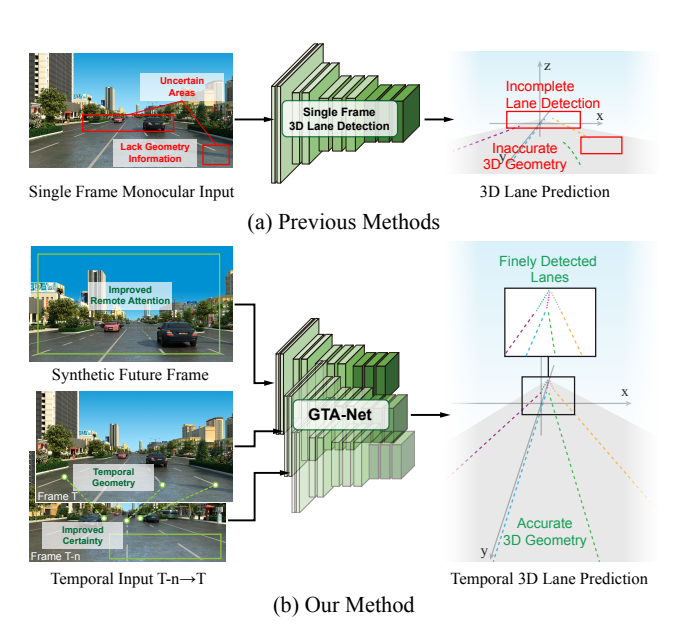


Figure 1. Comparison with Monocular 3D Lane Detection Approaches. (a) Existing methods [1, 3, 7, 10, 14] that rely on a single frame as input are hindered by inaccuracies in 3D geometry perception and difficulties in maintaining lane integrity. (b) In contrast, our approach, which incorporates multiple frames along with synthetic future frames, facilitates improved 3D geometric perception and enables integral lane detection within the scene.

with depth estimation [48], or by transforming features into a bird's-eye-view (BEV) representation [3, 7]. However, these approaches are built on fragile assumptions, like the reliance on highly accurate depth predictions or a flat-ground world, which often fail in complex real-world scenarios. More recent methods using 3D anchors or queries [14, 30] have shown promise, yet they still struggle with the fundamental ambiguity inherent in a single frame. This ambiguity manifests in two critical failures, as illustrated in Figure 1 (a): 1) inaccurate geometry, where predicted lanes deviate from their true 3D positions, and 2) broken lane integrity, where lanes, especially at a distance, are partially detected or missed entirely.

We argue that the key to overcoming these limitations lies not within the single frame, but in the *temporal evolution* of the scene. As a vehicle moves, the interplay be-

^{*}Equal contribution. †Corresponding author: Jianbing Shen.

tween consecutive frames contains powerful cues to resolve the aforementioned ambiguities. In this paper, we propose the Geometry-aware Temporal Aggregation Network (GTA-Net), a novel framework designed to systematically exploit this temporal information from complementary perspectives, as shown in Figure 1 (b).

First, to address the challenge of *inaccurate geometry*, we ask: *how can the past inform the present's geometry?* The relative motion between frames directly encodes the spatial relationships among scene elements. Inspired by this, we introduce the Temporal Geometry Enhancement Module (TGEM). By explicitly modeling the geometric consistency between past and present frames, TGEM learns to perceive depth-aware features, effectively correcting the geometric representation of the scene and leading to more accurate lane positioning.

Second, to tackle the problem of broken lane integrity, we ask: how can temporal context help us see ambiguous lanes? A lane that is faint or occluded now may have been clear in the past, or will become clear in the future. We therefore propose the Temporal Instance-aware Query Generation (TIQG) module. TIQG generates lane queries by aggregating instance information from both past and present views. More importantly, it addresses the challenge of detecting distant lanes with a novel strategy. As shown in Figure 4, a distant, undetectable lane becomes visible when the viewpoint moves closer. Since we cannot access real future frames, TIQG innovatively synthesizes a pseudo-future frame by digitally zooming into the region of interest. This allows us to generate effective queries for distant regions, dramatically improving lane integrity.

By seamlessly integrating these two components, GTA-Net leverages the temporal evolution to build a comprehensive understanding of the driving scene. Our main contributions are as follows:

- We propose the Geometry-aware Temporal Aggregation Network (GTA-Net), a novel architecture that systematically leverages temporal information to overcome the limitations of monocular 3D lane detection.
- We introduce the Temporal Geometry Enhancement Module (TGEM), which exploits geometric consistency across frames to learn depth-aware features for accurate 3D geometry perception.
- We present the Temporal Instance-aware Query Generation (TIQG) module, which enhances lane integrity by aggregating temporal instance cues.
- Extensive experiments show that GTA-Net achieves new state-of-the-art performance on the OpenLane benchmark, demonstrating its effectiveness and robustness across diverse and challenging scenarios.

2. Related Work

2.1. 2D Lane Detection

2D lane detection, a critical aspect of autonomous driving, strives to precisely determine the shapes and positions of lanes within images [40, 47]. With the development of deep learning [17, 49–51], deep neural network-based 2D lane detection has achieved remarkable strides forward [11, 16, 34, 42, 56]. According to the formulation of 2D lane detection, existing solutions can be divided into four categories: segmentation-based, anchor-based, keypoint-based and curve-based methods [14].

Segmentation-based approaches [18, 20, 55] employ segmentation tasks as intermediaries for executing lane detection. To be specific, these methods firstly complete pixel-wise classification to obtain 2D lane segmentation masks. Next, the segmentation masks are processed by some carefully-design strategies to construct a set of lanes. Anchor-based approaches primarily utilize line-like anchors for regressing offsets relative to ground truth lanes [15, 24, 33, 34, 38, 53]. To enhance the efficacy of lineshape anchors, row-based anchors have been devised for capitalizing on the natural shape of lanes [53]. By using row-based anchors, 2D lane detection task is converted into a row-wise classification problem. Furthermore, these row-based and column-based anchors are combined to reduce the occurrence of localization errors in side lanes [34]. Keypoint-based approaches offer a flexible framework for modeling lane positions [18, 35, 42]. At the outset, these methodologies embark on predicting the 2D coordinates of pivotal points along the lanes [18]. Following this initial step, a diverse array of strategies is employed to effectively group these key points into distinct lanes [42]. Curve-based approaches leverage a range of curve formulations to model lanes [6, 25, 39]. Specifically, this type of method aims to estimate the parameters of curves to obtain 2D lane detection results. BézierLaneNet [6] leverages the parametric Bézier curve for its computational simplicity, stability, and extensive flexibility in transformations. Additionally, the authors introduce a novel feature flip fusion module, which takes into account the symmetrical characteristics of lanes.

2.2. 3D Lane Detection

The objective of 3D lane detection is to identify lanes within 3D space and accurately estimate their coordinates [21, 31, 57]. In contrast to 2D lane detection, 3D lane detection methods need to perceive the geometric information of scenes. Some methodologies try to enhance perception accuracy by leveraging both lidar and camera data [28, 29]. However, the acquisition and annotation expenses associated with multi-modal data are prohibitively high, constraining the practical implementation of such methodologies. Hence, monocular 3D lane detection garners increased

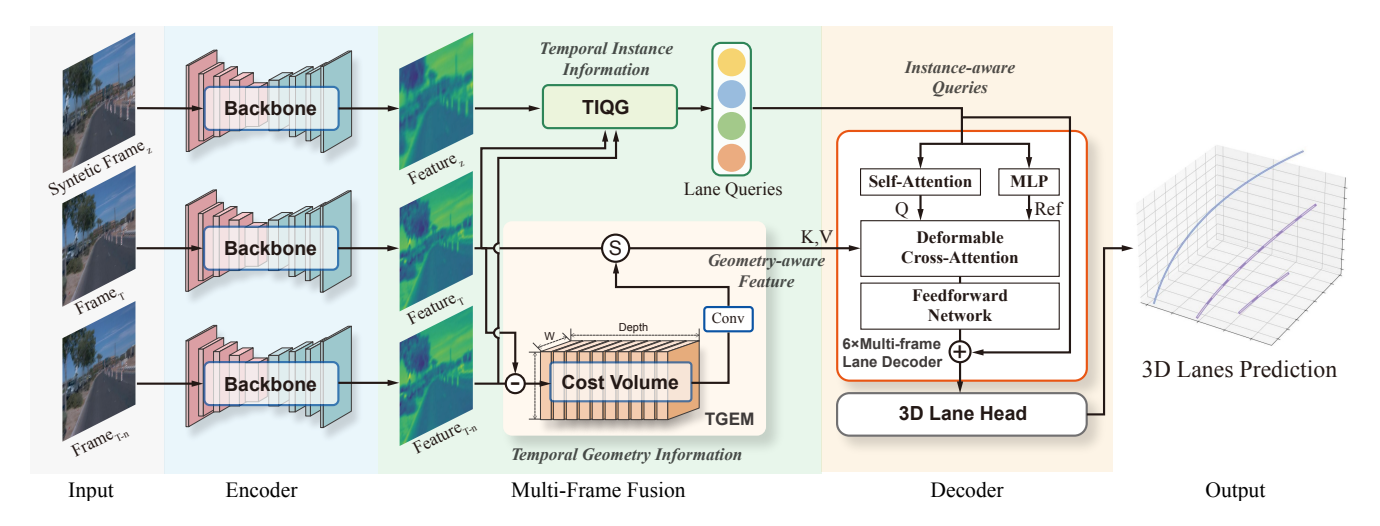


Figure 2. **Illustration of the Overall Architecture of the Proposed GTA-Net**. The input images are first fed into a backbone network to extract 2D perspective features. Next, TGEM is applied to enhance the geometric perception. Simultaneously, TIQG is used to generate lane queries. The lane queries and features are sent to the decoder to obtain 3D lane predictions.

interest due to its provision of a cost-effective alternative to multi-modal methodologies [31].

Monocular 3D lane detection is challenging due to the absence of depth information. To address this issue, SALAD [48] incorporates a depth prediction branch to estimate depth, which is used to project 2D lanes to 3D space. However, employing depth estimation in the process of detecting lanes may introduce cumulative errors and further exhibits inferior performance. IPM-based approaches have become increasingly prominent owing to their advantageous geometric properties for lane depiction in BEV perspective [31]. 3D-LaneNet [7] utilizes IPM for the conversion of FV features into BEV features, enabling bidirectional information flow between image-view and top-view representations. Next, these features are leveraged for learning the anchor offsets of lanes in the BEV space. Gen-LaneNet [10] introduces a novel lane anchor representation guided by geometry in a newly defined coordinate system, which employs a specific geometric transformation to directly compute real 3D lane points from the network output. It is essential to emphasize that aligning the lane points with the underlying top-view features in the newly defined coordinate frame is crucial for establishing a generalized method capable of effectively handling diverse scenes.

To overcome IPM's reliance on the flat-ground assumption [4], recent methods operate directly in 3D. Anchor3DLane [14], for instance, forgoes the BEV representation by regressing 3D anchors directly, which are then projected onto the image to extract features. LATR [30] uses a transformer-based architecture for monocular 3D lane detection. Specifically, the authors design a lane-aware query generator that produces queries derived from 2D lane segmentation. Besides, dynamic 3D ground PE generator is presented to embed 3D information during query updating.

3. Method

Our proposed Geometry-aware Temporal Aggregation Network (GTA-Net) leverages temporal evolution to address the core challenges of monocular 3D lane detection. This section details its architecture and key components. We first provide an overview of the entire GTA-Net framework. Then, we elaborate on our two core contributions: the Temporal Geometry Enhancement Module (TGEM) for better geometry perception, and the Temporal Instance-aware Query Generation (TIQG) for enhancing lane integrity. Finally, we describe the training objective and loss functions.

3.1. Overall Architecture

Given successive front-view images I_t and $I_{t-n} \in \mathbb{R}^{3 \times H \times W}$, the objective of monocular 3D lane detection is to estimate the 3D coordinates of the lane lines in the image I_t . Each 3D lane can be described by a set of 3D points along with the corresponding lane category:

$$L = (P, C), \quad P = (x_i, y_i, z_i)_{i=1}^N,$$
 (1)

where L denotes a 3D lane, C represents the corresponding lane category of L, P is composed of N 3D points with N being a predefined parameter. It is noted that the sequence $\{y_1, y^2, ..., y^N\}$ is often defined as a predetermined longitudinal coordinate [3, 7, 10]. Based on the above descriptions about lane representation, the 3D lanes in an input image I_t can be represented as $G = \{L^1, L^2, ..., L^M\}$, where G and M represent the collection and the number of 3D lanes, respectively.

The overall architecture of our GTA-Net is illustrated in figure 2. Initially, a 2D backbone network is utilized to extract image features F_t and F_{t-n} from the input front-view

images I_t and I_{t-n} :

$$F_t = \text{Backbone}(I_t), \quad F_{t-n} = \text{Backbone}(I_{t-n}), \quad (2)$$

where Backbone(\cdot) denotes transformation of the used 2D backbone network. Subsequently, the Temporal Geometry Enhancement Module (TGEM) takes these image features F_t and F_{t-n} as input to obtain geometry-aware features:

$$F_{ge} = TGEM(F_{t-n}, F_t), \tag{3}$$

where F_{ge} and TGEM(·) indicate geometry-aware features and the transformation of TGEM, respectively. TGEM aims to learn the geometric relationships between successive frames, thereby enhancing the depth perception capability of our GTA-Net in driving scenes. Simultaneously, image features F_t and F_{t-n} are sent to Temporal Instance-aware Query Generation (TIQG), which generates queries by making full use of temporal instance information. This process can be formulated as follows:

$$Q = \text{TIQG}(F_{t-n}, F_t), \tag{4}$$

where Q represents the generated instance-aware queries, and $TIQG(\cdot)$ denotes the transformation performed by the TIQG module. Next, the instance-aware queries Q and geometry-aware features F_{ge} are fed into a deformable attention [46, 58] based decoder to iteratively update queries:

$$Q_u = \text{Decoder}(Q, F_{qe}), \tag{5}$$

where Q_u and $\operatorname{Decoder}(\cdot)$ denote the updated queries and the transformation of the above deformable attention-based decoder, respectively. Finally, the updated queries Q_u are fed into the 3D lane detection head to output the predictions of 3D lanes in the input image I_t :

$$\hat{G} = \text{Head}(Q_u), \tag{6}$$

where \hat{G} indicates the estimated 3D lanes, and Head (\cdot) denotes 3D lane detection head. For the losses, we follow the setting of [30].

3.2. Temporal Geometry Enhancement Module

The inherent absence of depth cues in monocular input images poses a significant challenge for monocular 3D lane detection solutions. Without depth information, accurately understanding the complex geometric details of driving scenes becomes difficult. Drawing inspiration from prior research [44, 52] in monocular depth estimation, this study aims to alleviate this limitation by utilizing the geometric relationship between consecutive frames. To this end, we propose Temporal Geometry Enhancement Module (TGEM), which is designed to delve into the geometric consistency hidden in successive frames. The structure of

TGEM is described by figure 2. In detail, TGEM consists of three main stages: cost volume construction, geometric feature leaning, geometry-aware feature enhancement.

Cost volume construction. To uncover the potential geometric information within successive monocular images, we first construct a cost volume in the initial stage of TGEM. This is because the cost volume is capable of capturing the geometric relationship between adjacent frames [8].

Starting with 2D features F_t and F_{t-n} extracted from the 2D backbone network, we replicate these features D times along the depth dimension, where D represents a designated depth range. The process can be formulated as follows:

$$E_t = \operatorname{Repeat}(F_t), \quad E_{t-n} = \operatorname{Repeat}(F_{t-n}), \quad (7)$$

where E_t and E_{t-n} denote the expanded features, and Repeat (\cdot) represents the feature expanding operation. Next, the expanded features E_{t-n} in image coordinate system of t-n frame is projected onto image coordinate system of t frame by using camera intrinsics, extrinsics and lidar poses:

$$\hat{E}_t = \text{Warp}(F_{t-n}),\tag{8}$$

where \hat{E}_t denotes the warped features in image coordinate system of t frame, and $\mathrm{Warp}(\cdot)$ indicates the projection from image coordinate system of t-n frame to image coordinate system of t frame. In the final step, the matching cost between \hat{E}_t and E_t is computed by using l_1 norm:

$$C = \|\hat{E}_t - E_t\|_1,\tag{9}$$

where $\|\cdot\|_1$ denotes the transformation of l_1 norm, and C indicates the cost volume between the input successive front-view images I_t and I_{t-n} .

Geometric feature learning. Once the cost volume between successive front-view images is obtained, we utilize cascaded 2D convolution, batch normalization layer, and ReLU activation function to transform the cost volume into geometric features. This transformation can be expressed as follows:

$$F_g = \text{ReLU}(\text{BN}(\text{Conv}(C))), \tag{10}$$

where F_g denotes geometric features containing the 3D structural information of the driving scene, and $Conv(\cdot)$, $BN(\cdot)$ and $ReLU(\cdot)$ represent the transformation of 2D convolution, batch normalization layer and ReLU activation function, respectively.

Geometry-aware feature enhancement. To enrich the geometric perception capability of our GTA-Net, we aim to dynamically infuse geometric features into 2D features of t frame. To be specific, we first utilize geometric features F_g to derive two learnable tensors: weights α and residual β :

$$\alpha = \operatorname{Sigmoid}(\operatorname{BN}(\operatorname{Conv}(F_q))),\tag{11}$$

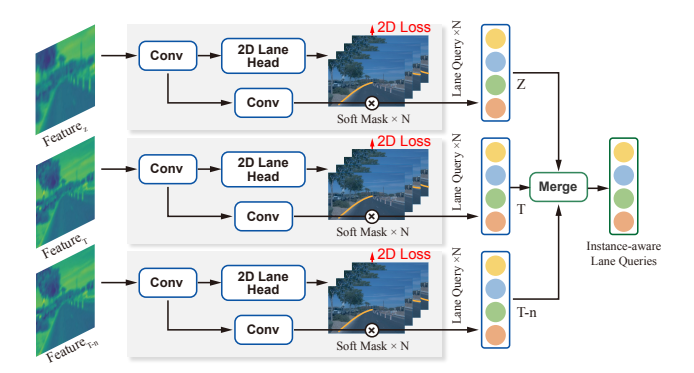


Figure 3. An Overview of the Proposed Temporal Instanceaware Query Generation (TIQG) Module. TIQG strategically integrates temporal cues into the query generation process, thereby enhancing its capacity to exploit temporal instance information for promoting lane integrity.

$$\beta = \text{ReLU}(\text{BN}(\text{Conv}(F_a))), \tag{12}$$

where Sigmoid(\cdot) denotes the transformation of sigmoid activation function. Subsequently, the weights α and residual β are used to inject geometric information into 2D features:

$$F_{qe} = \alpha F_t + \beta. \tag{13}$$

As a result, the feature enhancement mechanism enables our GTA-Net to dynamically adjust and integrate geometric information into the feature extraction process, thereby enhancing its ability to perceive intricate geometric structures within the scene.

3.3. Temporal Instance-aware Query Generation

While the TGEM module provides rich geometric context (what the scene looks like), it does not explicitly tell us where the lanes are. Accurately localizing all lanes, especially those that are distant or partially occluded, requires instance-level priors. Successive frames offer a wealth of such information: a lane barely visible now might have been clear seconds ago. To harness this rich temporal context, we propose the Temporal Instance-aware Query Generation (TIQG) module, as illustrated in Figure 3. The goal of TIQG is to generate a comprehensive and highly accurate set of lane queries by strategically aggregating information from the past, present, and a synthesized future. This process unfolds in three key stages: initial query generation from monocular frames, synthetic future query generation for distant lanes, and finally, temporal query aggregation.

Initial query generation. The initial query generation process involves generating temporal queries for both frame t and frame t-n. The queries consist of two-level embeddings: instance-level embeddings and point-level embeddings. To derive instance-level embedding, cascaded 2D convolutions are employed to process image features F_t and F_{t-n} as follows:

$$Q_t^l = \operatorname{Conv}(F_t), \quad Q_{t-n}^l = \operatorname{Conv}(F_{t-n}),$$
 (14)



Figure 4. Monocular Lane Detection Results of Setting Current and the Synthetic Future Frames as Input. The white line represents the predicted lane line and the red line denotes the gt. We see that the lane line is missing in the predictions when accepting the current frame. In contrast, there is a white line in the visual results for treating the synthetic future frame as input.

where Q_t^l and Q_{t-n}^l denote the generated instance-level embeddings of frame t and frame t-n, respectively. For point-level embedding, we define two learnable parameters Q_t^p and Q_{t-n}^p . Subsequently, these corresponding two-level embeddings are merged using the following formulation:

$$Q_t = Q_t^l \oplus Q_t^p, \quad Q_{t-n} = Q_{t-n}^l \oplus Q_{t-n}^p, \tag{15}$$

where \oplus represents the broadcasting summation.

Synthetic future query generation. As shown in figure 4, the 3D lane is not detected at the intersection, likely due to increased distance of the lane from the camera. To mitigate this issue, we seek to reduce the distance between the camera and the lane. A straightforward approach would involve using a future frame; however, real-world applications do not provide access to future information. As a solution, we synthesize a future frame by zooming in on the scene. This synthetic frame is then fed into the 3D lane detection model. Notably, we observe that lanes, which were initially undetected, become discernible in the synthetic future frame. This observation motivates the generation of pseudo-future frame to effectively detect lanes distant regions.

Based on the aforementioned analysis, we design the synthetic future query generation. Initially, we first crop and magnify the input image I_t to generate a synthetic future frame. Then, this synthetic future frame undergoes feature extraction to derive 2D perspective features F_p . Once the 2D perspective features F_p are obtained, the corresponding queries can be formulated as follows:

$$Q_p^l = \operatorname{Conv}(F_p), \quad Q_p = Q_p^l \oplus Q_p^p, \tag{16}$$

where Q_p denotes synthetic future queries, while Q_p^l and Q_p^p are instance-level embedding and point-level embedding, respectively. By integrating both instance-level and point-level embeddings, TIQG gains a comprehensive understanding of the distant context, enhancing its capability to detect 3D lanes in distant regions.

Temporal query aggregation. To fully explore temporal context, the information in these temporal queries Q_t , Q_{t-1} and Q_p are interacted by using cross-attention in the step of

Table 1. Quantitative Comparison of Monocular 3D Lane Detection Solutions on the OpenLane Dataset. \downarrow and \uparrow indicate that lower and higher values, respectively, signify superior performance. **Bold** numbers represent the best results. GTA-Net obtains the competitive performance on F1-score, lane category accuracy, x/z errors for both near and far range.

Methods	Year F1 (%		Category	X error (m) ↓		Z error (m) ↓	
		F1 (%) †	Accuracy (%)	near	far	near	far
3DLaneNet [7]	2019	44.1	-	0.479	0.572	0.367	0.443
GenLaneNet [10]	2020	32.3	-	0.593	0.494	0.140	0.195
Cond-IPM	-	36.6	-	0.563	1.080	0.421	0.892
Persformer [3]	2022	50.5	89.5	0.319	0.325	0.112	0.141
CurveFormer [1]	2023	50.5	-	0.340	0.772	0.207	0.651
BEV-LaneDet [43]	2022	58.4	-	0.309	0.659	0.244	0.631
Anchor3DLane [14]	2023	53.1	90.0	0.300	0.311	0.103	0.139
DecoupleLane [12]	2023	51.2	-	-	-	-	-
LaneCMK [54]	2024	55.8	89.2	0.310	0.303	0.083	0.123
GroupLane [22]	2024	60.2	91.6	0.371	0.476	0.220	0.357
CaliFree3DLane [9]	2024	56.4	-	0.319	0.767	0.245	0.706
CaliFree3DLane* [9]	2024	57.0	-	0.306	0.761	0.227	0.683
3DLaneFormer [5]	2024	55.0	89.9	0.283	0.305	0.106	0.138
DB3D-L [27]	2025	55.2	-	0.254	0.682	0.202	0.622
Freq-3DLane [36]	2025	59.7	-	0.265	0.665	0.196	0.608
CurveFormer++ [2]	2025	52.5	87.8	0.333	0.805	0.186	0.687
Ours	-	62.4	92.8	0.225	0.254	0.078	0.110

temporal query aggregation, which can be described by:

$$Q_p^u = \text{CA}(Q_p, Q_t), \quad Q_{t-1}^u = \text{CA}(Q_{t-1}, Q_t), \quad (17)$$

where Q_p^u , Q_{t-1}^u and $\mathrm{CA}(\cdot)$ denote the updated synthetic future queries, the updated queries of frame t-1 and the transformation of cross-attention. Subsequently, these lane queries are fed into cascaded convolutions to obtain instance-aware queries Q:

$$Q = \text{Conv}(\text{Concat}(Q_t, Q_{t-1}, Q_p)), \tag{18}$$

where $Concat(\cdot)$ denotes concatenation operation. The instance-aware queries integrate rich instance-aware information, thereby enhancing the capacity to comprehensively perceive lanes to promote lane integrity.

3.4. Loss Function

With the matched ground truth 3D lanes corresponding to the output 3D lane queries, we compute the loss for each respective pair. To be specific, L1 loss is employed to regress the *x*-coordinates and *z*-coordinates. Binary cross-entropy loss is used to enforce the visibility constraint of the output 3D lanes. Focal loss [23] is utilized to optimize the predicted lane category. In addition, a 2D segmentation loss is also included as an auxiliary loss. Hence, the final objective function of our GTA-Net can be formulated by:

$$\mathcal{L}_{total} = \mathcal{L}_{vis} + w_x \mathcal{L}_x + w_z \mathcal{L}_z + w_{cate} \mathcal{L}_{cate} + w_{seq} \mathcal{L}_{seq}.$$
(19)

where \mathcal{L}_{total} denotes the total loss, w_x , w_z , w_{cate} and w_{seg} are hyperparameters.

4. Experiments

This section provides a detailed overview of our experimental setup. We then evaluate the performance of our GTA-Net through a series of comparative analyses against state-of-the-art methods. Additionally, we present several ablation studies to gain a deeper understanding of the effectiveness of our proposed approach. Through these experiments, we aim to provide a thorough assessment of the capabilities and contributions of our model.

4.1. Experimental Setup

Dataset and Evaluation metrics. In the experiments, we use the OpenLane dataset [3], derived from the Waymo dataset [37], as a comprehensive benchmark for 3D lane detection. Comprising 1,000 segments and 200,000 frames, this dataset captures diverse environmental conditions such as varying weather, terrain, and lighting. The images in the OpenLane dataset have a resolution of 1280×1920 pixels and include 880,000 lane annotations spanning 14 categories. The OpenLane dataset provides a diverse and challenging set for evaluating 3D lane detection algorithms. We employ the official evaluation metrics to assess the effectiveness of our model on the OpenLane dataset. Specifically, we report the F1 score, lane category accuracy, and x/z errors in both the near and far ranges.

Implementation details. In our GTA-Net, we use ResNet-50 [13] as the 2D backbone network for extracting image features. Before feature extraction, all input images are resized to a resolution of 720×960. The experiments

Table 2. Quantitative Comparison of Monocular 3D Lane Detection Methods on the OpenLane Dataset Under Different Scenarios. Bold numbers denote the best results. "All" indicates the average value of F1 scores in all scenarios. The proposed GTA-Net achieves superior performance under various extremely challenging scenarios than other solutions.

Methods	Year	All	Up & Down	Curve	Extreme Weather	Night	Intersection	Merge & Split
3DLaneNet [7]	2019	44.1	40.8	46.5	47.5	41.5	32.1	41.7
GenLaneNet [10]	2020	32.3	25.4	33.5	28.1	18.7	21.4	31.0
Persformer [3]	2022	50.5	42.4	55.6	48.6	46.6	40.0	50.7
CurveFormer [1]	2023	50.5	45.2	56.6	49.7	49.1	42.9	45.4
BEV-LaneDet [43]	2022	58.4	48.7	63.1	53.4	53.4	50.3	53.7
Anchor3DLane [14]	2023	54.3	47.2	58.0	52.7	48.7	45.8	51.7
DecoupleLane [12]	2023	51.2	43.5	57.3	-	48.9	43.5	-
LATR [30] 3	2023	61.9	55.2	68.2	57.1	55.4	52.3	61.5
LaneCMK [54]	2024	55.8	47.3	58.6	53.2	48.0	42.2	51.7
CaliFree3DLane [9]	2024	56.4	48.7	60.4	54.7	51.9	49.5	51.8
CaliFree3DLane* [9]	2024	57.0	48.9	62.3	54.8	52.0	50.2	52.1
3DLaneFormer [5]	2024	55.0	49.0	58.3	54.5	50.4	46.3	52.3
Freq-3DLane [36]	2025	59.7	52.0	65.5	56.5	54.5	51.8	56.4
CurveFormer++ [2] 5	2025	52.7	48.3	59.4	50.6	48.4	45.0	48.1
Ours	-	62.4	55.5	68.3	57.5	56.8	52.7	61.8

are conducted on the PyTorch platform using a workstation equipped with eight Tesla A100 GPUs, each with 40 GB of memory. For optimization, we employ the AdamW optimizer with a weight decay of 0.01. The initial learning rate is set to $2e^{-4}$, and a cosine annealing scheduler is applied to gradually adjust the learning rate. Our model is trained for 24 epochs, with a batch size of 64. Additionally, we set $w_x=2,\,w_z=10,\,w_{cate}=10$ and $w_{seg}=5$.

Compared methods. We compare our GTA-Net with the following monocular 3D detection methods: 3DLaneNet [7], Gen-LaneNet [10], PersFormer [3], Cond-IPM, Curve-Former [1], DecoupleLane [12], Anchor3DLane [14], BEV-LaneDet [43], LATR [30], GroupLane [22], LaneCMK [54], CaliFree3DLane* [9], LaneCPP [32], 3DLaneFormer [5], DB3D-L [27], Freq-3DLane [36] and CurveFormer++ [2].

4.2. Main Results

Quantitative results. We present a comprehensive quantitative evaluation of our proposed GTA-Net on the challenging OpenLane dataset, with detailed results summarized in Table 1. The experimental findings unequivocally demonstrate that GTA-Net achieves superior performance, setting a new SoTA benchmark for monocular 3D lane detection.

Specifically, GTA-Net excels across key evaluation metrics. It attains the highest F1 score, indicative of its robust ability to precisely identify 3D lanes while effectively balancing recall and precision to minimize both missed detections and false positives. Furthermore, our method exhibits superior lane category accuracy, underscoring its enhanced capability in semantically understanding and classifying diverse lane types. Beyond detection, GTA-Net also demonstrated.

strates exceptional localization precision. It consistently yields the smallest x and z errors across both near and far perception ranges, a critical validation of its effectiveness in accurately estimating the spatial coordinates of 3D lanes, irrespective of their distance from the ego-vehicle. These results collectively affirm the robustness and practical utility of GTA-Net in complex scenarios.

To further validate the effectiveness of the proposed GTA-Net, we present results across a range of challenging scenarios. Table 2 reports the 3D lane detection performance under different conditions, measured by the F1 score. Notably, our method outperforms existing approaches, achieving the highest F1 score across all scenarios. This demonstrates the robustness of our model in handling diverse driving environments, underscoring its reliability and efficacy in accurately detecting 3D lanes under varying real-world conditions.

Visual Results. Beyond quantitative metrics, a rigorous qualitative assessment is crucial for a comprehensive understanding of GTA-Net's performance. To this end, we present a series of visualization results on the challenging OpenLane dataset, offering an intuitive insight into our model's capabilities. As vividly depicted in Figure 5, GTA-Net consistently demonstrates an exceptional ability to accurately detect 3D lanes directly within the complex input images. More importantly, it precisely estimates their corresponding positions in 3D space, even under varying scene conditions. These visual outcomes not only corroborate the superior quantitative performance but also powerfully illustrate the model's robustness and accuracy in real-world scenarios, affirming its excellent capacity for both identifying and accurately localizing lanes in 3D space.



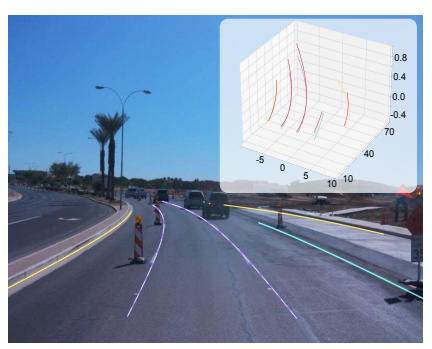




Figure 5. **Illustration of Predicted 3D Lanes on the OpenLane Dataset.** We present the predicted 3D lanes in both the perspective view and the 3D spatial representation. The red lines denote the ground truth lanes, while the other colored lines represent the predicted lanes.

Table 3. **Ablation study of the proposed modules.** We evaluate the effect of TGEM and TIQG by ablating them.

Methods	F1 (%)	X erro	or (m)	Z error (m)		
wichiods	11 (70)	near	far	near	far	
Baseline	61.7	0.235	0.273	0.085	0.120	
w/o. TGEM	62.1	0.229	0.257	0.081	0.112	
w/o. TIQG	62.1	0.229	0.264	0.080	0.114	
w/o. Cost Volume	62.2	0.228	0.256	0.080	0.112	
Ours	62.4	0.225	0.254	0.078	0.110	

4.3. Ablation Studies

We design a series of meticulous experiments to evaluate the efficacy of our approach in addressing the inherent challenges of monocular 3D lane detection. These experiments are carefully structured to provide a comprehensive understanding of how the proposed techniques contribute to improving overall performance.

Effect of TGEM. To systematically dissect the contributions of individual components within our proposed GTA-Net framework, we first conduct an ablation study focusing on the Temporal Geometry Enhancement Module (TGEM). As detailed in Table 3, we evaluate the performance of a modified GTA-Net variant, denoted as *w/o*. TGEM, where the TGEM module is deliberately omitted. The comparative results reveal a marked and consistent degradation in performance across all evaluated metrics when TGEM is excluded. This significant decline unequivocally highlights the critical and indispensable role of TGEM. It actively promotes the network's ability to accurately capture and robustly leverage intricate geometric cues from the temporal evolution of the scene, which are crucial for resolving ambiguities inherent in monocular 3D lane detection.

Effect of TIQG. We next evaluate the contribution of the TIQG module. As presented in Table 3, the variant labeled *w/o*. TIQG corresponds to a version of GTA-Net where the TIQG module is omitted. The results reveal a signif-

icant degradation in performance across all metrics when TIQG is excluded, thereby suggesting its critical role in effectively leveraging temporal cues. This demonstrates the importance of TIQG in improving the accuracy of 3D lane detection from monocular inputs by harnessing temporal instance information to enhance the integrity of lanes.

Effect of Cost Volume. To investigate the contribution of the cost volume construction within TGEM, we conduct an ablation study where this component is omitted. In this variant, referred to as w/o. Cost Volume, the geometric feature learning directly processes the concatenated raw 2D features without an explicit cost volume generation step. As shown in Table 3, the removal of the cost volume leads to a degradation in performance across all metrics. This suggests that while cost volume plays a role in capturing precise geometric relationships between frames. The cost volume provides a fine-grained inter-frame geometric correspondence that aids in depth-aware feature generation, and its absence impacts the overall accuracy.

5. Conclusion

In this paper, we tackle two key challenges in monocular 3D lane detection: the inaccurate geometric information of predicted 3D lanes and the difficulty in detecting remote lanes. To address these issues, we propose a novel Geometryaware Temporal Aggregation Network (GTA-Net) by harnessing temporal evolution for monocular 3D lane detection. We introduce the Temporal Geometry Enhancement Module (TGEM), which leverages geometric consistency across successive frames to enhance depth perception and improve geometric understanding of the scene. Additionally, we present the Temporal Instance-aware Query Generation (TIQG) module, which strategically incorporates temporal context into the query generation process, enabling a more comprehensive exploration of instance-aware information across frames. Through extensive and rigorous experimentation, the results demonstrate that the proposed GTA-Net outperforms existing methods.

References

- [1] Yifeng Bai, Zhirong Chen, Zhangjie Fu, Lang Peng, Pengpeng Liang, and Erkang Cheng. Curveformer: 3d lane detection by curve propagation with curve queries and attention. In *IEEE International Conference on Robotics and Automation*, 2023, 1, 6, 7
- [2] Yifeng Bai, Zhirong Chen, Pengpeng Liang, Bo Song, and Erkang Cheng. Curveformer++: 3d lane detection by curve propagation with temporal curve queries and attention. *IEEE Transactions on Intelligent Transportation Systems*, 2025. 6, 7
- [3] Li Chen, Chonghao Sima, Yang Li, Zehan Zheng, Jiajie Xu, Xiangwei Geng, Hongyang Li, Conghui He, Jianping Shi, Yu Qiao, et al. Persformer: 3d lane detection via perspective transformer and the openlane benchmark. In *European Conference on Computer Vision*, 2022. 1, 3, 6, 7
- [4] Ziye Chen, Kate Smith-Miles, Bo Du, Guoqi Qian, and Mingming Gong. An efficient transformer for simultaneous learning of bev and lane representations in 3d lane detection. arXiv preprint arXiv:2306.04927, 2023. 3
- [5] Kun Dong, Jian Xue, Xing Lan, and Ke Lu. 3dlaneformer: Rethinking learning views for 3d lane detection. In *IEEE International Conference on Image Processing*, 2024. 6, 7
- [6] Zhengyang Feng, Shaohua Guo, Xin Tan, Ke Xu, Min Wang, and Lizhuang Ma. Rethinking efficient lane detection via curve modeling. In *Proceedings of the IEEE/CVF Confer*ence on Computer Vision and Pattern Recognition, 2022. 2
- [7] Noa Garnett, Rafi Cohen, Tomer Pe'er, Roee Lahav, and Dan Levi. 3d-lanenet: end-to-end 3d multiple lane detection. In Proceedings of the IEEE/CVF International Conference on Computer Vision, 2019. 1, 3, 6, 7
- [8] Xiaodong Gu, Zhiwen Fan, Siyu Zhu, Zuozhuo Dai, Feitong Tan, and Ping Tan. Cascade cost volume for high-resolution multi-view stereo and stereo matching. In *Proceedings of* the IEEE/CVF Conference on Computer Vision and Pattern Recognition, 2020. 4
- [9] Weizhi Guo, Chaochao Li, Kaijiang Li, Pei Lv, and Mingliang Xu. Califree3dlane: Calibration free spatio-temporal bev representation for monocular 3d lane detection. *IEEE Transactions on Intelligent Transportation Systems*, 2024. 6, 7
- [10] Yuliang Guo, Guang Chen, Peitao Zhao, Weide Zhang, Jinghao Miao, Jingao Wang, and Tae Eun Choe. Gen-lanenet: A generalized and scalable approach for 3d lane detection. In European Conference on Computer Vision, 2020. 1, 3, 6, 7
- [11] Jianhua Han, Xiajun Deng, Xinyue Cai, Zhen Yang, Hang Xu, Chunjing Xu, and Xiaodan Liang. Laneformer: Object-aware row-column transformers for lane detection. In *Proceedings of the AAAI conference on artificial intelligence*, 2022. 2
- [12] Wencheng Han and Jianbing Shen. Decoupling the curve modeling and pavement regression for lane detection. arXiv preprint arXiv:2309.10533, 2023. 6, 7
- [13] Kaiming He, Xiangyu Zhang, Shaoqing Ren, and Jian Sun. Deep residual learning for image recognition. In *Proceedings of the IEEE conference on computer vision and pattern recognition*, 2016. 6

- [14] Shaofei Huang, Zhenwei Shen, Zehao Huang, Zi-han Ding, Jiao Dai, Jizhong Han, Naiyan Wang, and Si Liu. Anchor3dlane: Learning to regress 3d anchors for monocular 3d lane detection. In Proceedings of the IEEE/CVF Conference on Computer Vision and Pattern Recognition, 2023. 1, 2, 3, 6, 7
- [15] Dongkwon Jin, Wonhui Park, Seong-Gyun Jeong, Heeyeon Kwon, and Chang-Su Kim. Eigenlanes: Data-driven lane descriptors for structurally diverse lanes. In *Proceedings of the IEEE/CVF Conference on Computer Vision and Pattern Recognition*, 2022. 2
- [16] Dongkwon Jin, Dahyun Kim, and Chang-Su Kim. Recursive video lane detection. In Proceedings of the IEEE/CVF International Conference on Computer Vision, 2023.
- [17] Alexander Kirillov, Eric Mintun, Nikhila Ravi, Hanzi Mao, Chloe Rolland, Laura Gustafson, Tete Xiao, Spencer Whitehead, Alexander C Berg, Wan-Yen Lo, et al. Segment anything. In Proceedings of the IEEE/CVF International Conference on Computer Vision, 2023. 2
- [18] Yeongmin Ko, Younkwan Lee, Shoaib Azam, Farzeen Munir, Moongu Jeon, and Witold Pedrycz. Key points estimation and point instance segmentation approach for lane detection. *IEEE Transactions on Intelligent Transportation* Systems, 2021. 2
- [19] Qi Li, Yue Wang, Yilun Wang, and Hang Zhao. Hdmapnet: An online hd map construction and evaluation framework. In *International Conference on Robotics and Automa*tion, 2022. 1
- [20] Xuelong Li, Zhiyuan Zhao, and Qi Wang. Abssnet: Attention-based spatial segmentation network for traffic scene understanding. *IEEE Transactions on Cybernetics*, 2021. 2
- [21] Zhuoling Li, Chunrui Han, Zheng Ge, Jinrong Yang, En Yu, Haoqian Wang, Xiangyu Zhang, and Hengshuang Zhao. Grouplane: End-to-end 3d lane detection with channel-wise grouping. *IEEE Robotics and Automation Letters*, 2024. 2
- [22] Zhuoling Li, Chunrui Han, Zheng Ge, Jinrong Yang, En Yu, Haoqian Wang, Xiangyu Zhang, and Hengshuang Zhao. Grouplane: End-to-end 3d lane detection with channel-wise grouping. *IEEE Robotics and Automation Letters*, 2024. 6,
- [23] Tsung-Yi Lin, Priya Goyal, Ross Girshick, Kaiming He, and Piotr Dollár. Focal loss for dense object detection. In Proceedings of the IEEE international conference on computer vision, 2017. 6
- [24] Lizhe Liu, Xiaohao Chen, Siyu Zhu, and Ping Tan. Condlanenet: a top-to-down lane detection framework based on conditional convolution. In *Proceedings of the IEEE/CVF* international conference on computer vision, 2021. 2
- [25] Ruijin Liu, Zejian Yuan, Tie Liu, and Zhiliang Xiong. Endto-end lane shape prediction with transformers. In Proceedings of the IEEE/CVF winter conference on applications of computer vision, 2021. 2
- [26] Yicheng Liu, Tianyuan Yuan, Yue Wang, Yilun Wang, and Hang Zhao. Vectormapnet: End-to-end vectorized hd map learning. In *International Conference on Machine Learning*, 2023.

- [27] Yehao Liu, Xiaosu Xu, Zijian Wang, and Yiqing Yao. Db3d-l: Depth-aware bev feature transformation for accurate 3d lane detection. *arXiv* preprint arXiv:2505.13266, 2025. 6, 7
- [28] Yueru Luo, Xu Yan, Chaoda Zheng, Chao Zheng, Shuqi Mei, Tang Kun, Shuguang Cui, and Zhen Li M[^]. M[^]2-3dlanenet: Multi-modal 3d lane detection. arXiv preprint arXiv:2209.05996, 2022. 2
- [29] Yueru Luo, Shuguang Cui, and Zhen Li. Dv-3dlane: End-toend multi-modal 3d lane detection with dual-view representation. In *International Conference on Learning Representa*tions, 2023. 2
- [30] Yueru Luo, Chaoda Zheng, Xu Yan, Tang Kun, Chao Zheng, Shuguang Cui, and Zhen Li. Latr: 3d lane detection from monocular images with transformer. In *Proceedings of the IEEE/CVF International Conference on Computer Vision*, 2023. 1, 3, 4, 7
- [31] Fulong Ma, Weiqing Qi, Guoyang Zhao, Linwei Zheng, Sheng Wang, and Ming Liu. Monocular 3d lane detection for autonomous driving: Recent achievements, challenges, and outlooks. *arXiv preprint arXiv:2404.06860*, 2024. 1, 2,
- [32] Maximilian Pittner, Joel Janai, and Alexandru P Condurache. Lanecpp: Continuous 3d lane detection using physical priors. In Proceedings of the IEEE/CVF Conference on Computer Vision and Pattern Recognition, 2024. 7
- [33] Zequn Qin, Huanyu Wang, and Xi Li. Ultra fast structureaware deep lane detection. In European Conference on Computer Vision, 2020. 2
- [34] Zequn Qin, Pengyi Zhang, and Xi Li. Ultra fast deep lane detection with hybrid anchor driven ordinal classification. *IEEE Transactions on Pattern Analysis and Machine Intel*ligence, 2022. 2
- [35] Zhan Qu, Huan Jin, Yang Zhou, Zhen Yang, and Wei Zhang. Focus on local: Detecting lane marker from bottom up via key point. In *Proceedings of the IEEE/CVF Conference on Computer Vision and Pattern Recognition*, 2021. 2
- [36] Yongchao Song, Jiping Bi, Lijun Sun, Zhaowei Liu, Yahong Jiang, and Xuan Wang. Freq-3dlane: 3d lane detection from monocular images via frequency-aware feature fusion. *IEEE Transactions on Intelligent Transportation Systems*, 2025. 6,
- [37] Pei Sun, Henrik Kretzschmar, Xerxes Dotiwalla, Aurelien Chouard, Vijaysai Patnaik, Paul Tsui, James Guo, Yin Zhou, Yuning Chai, Benjamin Caine, et al. Scalability in perception for autonomous driving: Waymo open dataset. In Proceedings of the IEEE/CVF Conference on Computer Vision and Pattern Recognition, 2020. 6
- [38] Lucas Tabelini, Rodrigo Berriel, Thiago M Paixao, Claudine Badue, Alberto F De Souza, and Thiago Oliveira-Santos. Keep your eyes on the lane: Real-time attention-guided lane detection. In *Proceedings of the IEEE/CVF Conference on Computer Vision and Pattern Recognition*, 2021. 2
- [39] Lucas Tabelini, Rodrigo Berriel, Thiago M Paixao, Claudine Badue, Alberto F De Souza, and Thiago Oliveira-Santos. Polylanenet: Lane estimation via deep polynomial regression. In *International Conference on Pattern Recognition*, 2021. 2

- [40] Jigang Tang, Songbin Li, and Peng Liu. A review of lane detection methods based on deep learning. *Pattern Recogni*tion, 2021. 2
- [41] Jin Wang, Stefan Schroedl, Klaus Mezger, Roland Ortloff, Armin Joos, and Thomas Passegger. Lane keeping based on location technology. *IEEE Transactions on Intelligent Trans*portation Systems, 2005. 1
- [42] Jinsheng Wang, Yinchao Ma, Shaofei Huang, Tianrui Hui, Fei Wang, Chen Qian, and Tianzhu Zhang. A keypoint-based global association network for lane detection. In *Proceedings of the IEEE/CVF Conference on Computer Vision and Pattern Recognition*, 2022. 2
- [43] Ruihao Wang, Jian Qin, Kaiying Li, Yaochen Li, Dong Cao, and Jintao Xu. Bev-lanedet: a simple and effective 3d lane detection baseline. In Proceedings of the IEEE/CVF Conference on Computer Vision and Pattern Recognition, 2023. 6,
- [44] Jamie Watson, Oisin Mac Aodha, Victor Prisacariu, Gabriel Brostow, and Michael Firman. The temporal opportunist: Self-supervised multi-frame monocular depth. In Proceedings of the IEEE/CVF Conference on Computer Vision and Pattern Recognition, 2021. 4
- [45] Kyle R Williams, Rachel Schlossman, Daniel Whitten, Joe Ingram, Srideep Musuvathy, James Pagan, Kyle A Williams, Sam Green, Anirudh Patel, Anirban Mazumdar, et al. Trajectory planning with deep reinforcement learning in high-level action spaces. *IEEE Transactions on Aerospace and Elec*tronic Systems, 2022. 1
- [46] Zhuofan Xia, Xuran Pan, Shiji Song, Li Erran Li, and Gao Huang. Vision transformer with deformable attention. In Proceedings of the IEEE/CVF Conference on Computer Vision and Pattern Recognition, 2022. 4
- [47] Hang Xu, Shaoju Wang, Xinyue Cai, Wei Zhang, Xiaodan Liang, and Zhenguo Li. Curvelane-nas: Unifying lanesensitive architecture search and adaptive point blending. In Computer Vision–ECCV 2020: 16th European Conference, Glasgow, UK, August 23–28, 2020, Proceedings, Part XV 16, 2020. 2
- [48] Fan Yan, Ming Nie, Xinyue Cai, Jianhua Han, Hang Xu, Zhen Yang, Chaoqiang Ye, Yanwei Fu, Michael Bi Mi, and Li Zhang. Once-3dlanes: Building monocular 3d lane detection. In *Proceedings of the IEEE/CVF Conference on Computer Vision and Pattern Recognition*, 2022. 1, 3
- [49] Tianyi Yan, Wencheng Han, Xia Zhou, Xueyang Zhang, Kun Zhan, Cheng-zhong Xu, and Jianbing Shen. Rlgf: Reinforcement learning with geometric feedback for autonomous driving video generation. arXiv preprint arXiv:2509.16500, 2025.
- [50] Tianyi Yan, Dongming Wu, Wencheng Han, Junpeng Jiang, Xia Zhou, Kun Zhan, Cheng-zhong Xu, and Jianbing Shen. Drivingsphere: Building a high-fidelity 4d world for closedloop simulation. In *Proceedings of the Computer Vision and Pattern Recognition Conference*, 2025.
- [51] Tianyi Yan, Junbo Yin, Xianpeng Lang, Ruigang Yang, Cheng-Zhong Xu, and Jianbing Shen. Olidm: Object-aware lidar diffusion models for autonomous driving. In *Proceedings of the AAAI Conference on Artificial Intelligence*, 2025.

- [52] Jiayu Yang, Wei Mao, Jose M Alvarez, and Miaomiao Liu. Cost volume pyramid based depth inference for multi-view stereo. In Proceedings of the IEEE/CVF Conference on Computer Vision and Pattern Recognition, 2020. 4
- [53] Seungwoo Yoo, Hee Seok Lee, Heesoo Myeong, Sungrack Yun, Hyoungwoo Park, Janghoon Cho, and Duck Hoon Kim. End-to-end lane marker detection via row-wise classification. In Proceedings of the IEEE/CVF Conference on Computer Vision and Pattern Recognition workshops, 2020. 2
- [54] Runkai Zhao, Heng Wang, and Weidong Cai. Lanecmkt: Boosting monocular 3d lane detection with cross-modal knowledge transfer. In *Proceedings of the 32nd ACM In*ternational Conference on Multimedia, 2024. 6, 7
- [55] Tu Zheng, Hao Fang, Yi Zhang, Wenjian Tang, Zheng Yang, Haifeng Liu, and Deng Cai. Resa: Recurrent feature-shift aggregator for lane detection. In *Proceedings of the AAAI Conference on Artificial Intelligence*, 2021. 2
- [56] Tu Zheng, Yifei Huang, Yang Liu, Wenjian Tang, Zheng Yang, Deng Cai, and Xiaofei He. Clrnet: Cross layer refinement network for lane detection. In *Proceedings of* the IEEE/CVF Conference on Computer Vision and Pattern Recognition, 2022. 2
- [57] Zewen Zheng, Xuemin Zhang, Yongqiang Mou, Xiang Gao, Chengxin Li, Guoheng Huang, Chi-Man Pun, and Xiaochen Yuan. Pvalane: Prior-guided 3d lane detection with viewagnostic feature alignment. In Proceedings of the AAAI Conference on Artificial Intelligence, 2024. 2
- [58] Xizhou Zhu, Weijie Su, Lewei Lu, Bin Li, Xiaogang Wang, and Jifeng Dai. Deformable detr: Deformable transformers for end-to-end object detection. *arXiv preprint arXiv:2010.04159*, 2020. 4